

Interfacial activity of AuC6 nanoparticles using the pendant drop technique.

Miguel Ángel Fernández-Rodríguez^{1,*}, Yang Song², Miguel Ángel Rodríguez-Valverde¹,
Shaowei Chen², Miguel Ángel Cabrerizo-Vílchez¹ and Roque Hidalgo-Álvarez¹

¹*Biocolloid and Fluid Physics Group,
Applied Physics Department, Faculty of Sciences,
University of Granada, 18071 Granada (Spain)*

²*Department of Chemistry and Biochemistry,
University of California, 1156 High Street,
Santa Cruz, CA 95064 (USA)
rhidalgo@ugr.es*

The structure and orientation of nanoparticles at the liquid-liquid interface may be useful for the preparation of robust, self-assembled structures, devices, and membranes. The pendant drop technique enables to study the interfacial activity of nanoparticles with smaller amounts and upon more controlled conditions than with the traditional Langmuir film balance technique. The pendant drop technique was applied to characterize the interfacial activity of 2 nm-diameter AuC6 nanoparticles. The AuC6 nanoparticles in tetrahydrofuran solution deposited at the water/air interface described a violent adsorption process as the tetrahydrofuran was evaporated. Growing and shrinking experiments for the water/air and water/decane interfaces enabled to explore the arrangement of the AuC6 nanoparticles at each interface. A simply scaled particle theory of hard disks model was in agreement with the experimental data.

Keywords: Pendant drop; Interfacial activity; Nanoparticles; Water/air interface; Water/oil interface.

I. INTRODUCTION

The Langmuir film balance is a technique widely used to study the arrangement and interfacial activity of nanoparticles at water/air and water/oil interfaces¹⁻³. It is further used to synthesize nanoparticles with interfacial activity^{4,5}. On the other hand, the pendant drop tensiometer is usually used to characterize the diffusion of nanoparticles from bulk toward the interface^{6,7}. Due to the interface geometry and sample size in both techniques, the pendant drop technique enables to study the interfacial activity of nanoparticles with smaller amounts and upon more controlled conditions than with the traditional Langmuir film balance technique. Also, the pendant drop technique enables the study of interfacial dilatational rheology and subphase exchange when a coaxial double capillary is used⁸.

Diffusion of alkanethiol-capped gold nanoparticles from the oil phase to the interface is studied by pendant drop technique due to the colloidal stability of these nanoparticles⁶. When the nanoparticle diameter is in the range of a few nanometers, the adsorption energy of the nanoparticles at the interface is of the order of $k_B T$, thus the nanoparticles are expected to leave the interface due to thermal fluctuations⁶. The pendant drop technique has been proven to study complex systems as Janus cylinders which exhibit strong interfacial activity with different adsorption regimes⁷.

Direct deposition of nanoparticles at the interface of a pendant drop from a volatile solvent produces a violent

process in which solvent evaporation helps the nanoparticles to be adsorbed at the interface faster than the slower process of diffusion from the bulk toward the interface⁹. Also, this procedure allows to precisely control the amount of nanoparticles that are deposited at the interface.

There are several models that intend to explain the behavior of the nanoparticles at liquid/liquid interfaces. The simplest attempt is the hard disk model in which the nanoparticles are modeled like hard entities placed at the interface. The nanoparticles behave as hard disks without interaction when there is room enough for every nanoparticle but become a close-packed arrangement when the area per nanoparticle is decreased¹⁰. Nevertheless, if the particles were charged, it should be considered the repulsion between like-charged particles¹¹. On the other hand, Montecarlo simulations and experimental data of nanoparticles functionalized with large polymers exhibit a complex behavior compared to hard objects at liquid/liquid interfaces¹².

In this study, we characterized the interfacial activity of 2 nm-diameter gold nanoparticles capped with hexanethiol at the water/air and water/decane interfaces by the growing and shrinking pendant drop technique. The nanoparticles dispersed in a volatile solvent were directly deposited at the water/air interface using a microsyringe. The different arrangements of the nanoparticles at the interface were explored by changing the drop volume, thus the interface area available was changed for a fixed amount of nanoparticles.

II. MATERIALS AND METHODS

A. Sample preparation

The Brust protocol¹³ was used for the synthesis of gold homogeneous nanoparticles capped with hexanethiol (AuC6-NPs). Next, the fraction of 2 nm-diameter nanoparticles was selected by fractionation^{4,5}. The nanoparticles were redispersed in tetrahydrofuran (THF, Sigma Aldrich) and the final concentration was $1.7 \cdot 10^{12}$ AuC6-NPs per $1 \mu\text{l}$ of THF solution.

B. Electrophoretic mobility

The electrophoretic mobility of the AuC6-NPs was measured with a Malvern Zetasizer Nano (Malvern) device. It was measured at 25°C in MilliQ water ($-1.4 \pm 1.2 \cdot 10^{-8} \text{ m}^2/(\text{V} \cdot \text{s})$) and in sodium citrate (Sigma Aldrich) at 10^{-2} M concentration ($-1.1 \pm 0.7 \cdot 10^{-8} \text{ m}^2/(\text{V} \cdot \text{s})$).

C. Growing and shrinking pendant drop

The pendant drop technique consists in increasing and decreasing the volume of a MilliQ water pendant drop with the AuC6-NPs deposited at the interface. Real time drop images are processed at each step of volume variation and the drop area and surface tension are calculated by Axisymmetric Drop Shape Analysis Profile (ADSA-P)¹⁴. The pendant drop technique can explore the interfacial activity of nanoparticles at the water/air and water/oil interfaces. In this study, the oil phase studied was decane (Sigma Aldrich). THF was used as spreading solvent and $5 \mu\text{l}$ of THF deposited at a water pendant drop were fully evaporated (i.e. recovered the initial surface tension) after 350 s. For that reason, we waited twice this time to ensure that there was no presence of THF in all depositions.

Each pendant drop experiment involves two stages:

- First stage: deposition of the desired amount of AuC6-NPs in THF solution onto the surface of a $5 \mu\text{l}$ MilliQ water pendant drop in air with a $5 \mu\text{l}$ microsyringe (Hamilton) and a micropositioner (Fig. 1a). While the THF was evaporating, the volume of the pendant drop was slowly increased at $0.08 \mu\text{l/s}$ up to the final $20 \mu\text{l}$ volume and maintained until the surface tension was stable.
- Second stage: growing and shrinking the water/air or water/decane interface.

* Water/air interface: the shrinking and growing volume rate was $0.08 \mu\text{l/s}$ and the volume range was $20 \mu\text{l} \leftrightarrow 10 \mu\text{l}$, the shrinking was repeated 3 times and the growing twice (Fig.1b).

* Water/decane interface: first the pendant drop was placed inside the oil phase but with a volume of $5 \mu\text{l}$ to avoid the fall of the drop when it was immersed in the decane phase. Next the pendant drop was grown up to $30 \mu\text{l}$ and the process was repeated like for water/air case but with drop volumes between $30 \mu\text{l} \leftrightarrow 10 \mu\text{l}$ (Fig.1c).

The surface pressure $\Pi = \gamma_0 - \gamma$, where γ_0 is the surface tension of the phase without nanoparticles and γ is the measured surface tension, is plotted against the area of the pendant drop divided by the deposited AuC6-NPs number. Due to the low hysteresis of the growing/shrinking cycles, within the order of resolution of the technique, the cycles were averaged for each AuC6-NPs concentration.

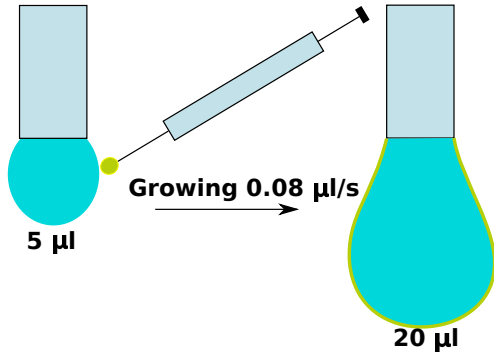
III. RESULTS AND DISCUSSION

Growing and shrinking pendant drop experiments were performed for water/air and water/decane interfaces and for different AuC6-NPs concentrations directly deposited at the interface as described in the Section II C. For the first stage of the pendant drop experiments the surface tension was plotted against time for different AuC6-NPs concentrations in Fig. 2. After the deposition of the AuC6-NPs onto the initial $5 \mu\text{l}$ water drop, the surface tension strongly decreased because of the surfactant effect of THF at the interface. After the THF evaporation the surface tension remained constant over time. A decrease in the final surface tension was observed as the AuC6-NPs concentration was increased for the same drop area (the area corresponding to a final $20 \mu\text{l}$ pendant drop, as described in Section II C). It can also be noticed a change in the pendant drop opacity as the AuC6-NPs concentration was increased (see Fig. 3).

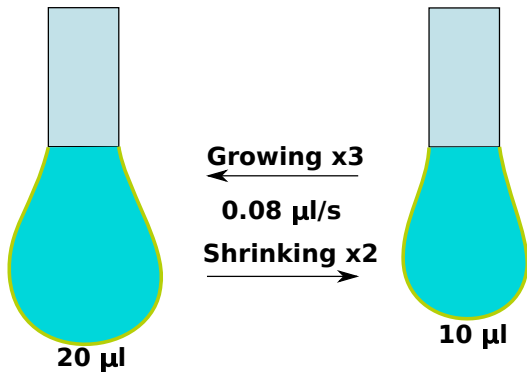
Although the 2 nm-diameter AuC6-NPs were expected to desorb from the interfaces due to thermal fluctuations⁶, in our experiments the AuC6-NPs exhibited a significant and stable effect on the surface tension after the THF evaporation. Moreover, the surface tension was lower as the AuC6-NPs number was increased (see Fig. 2). These evidences are pointing out that the AuC6-NPs interface coverage is stable and that the thermal fluctuations are not forcing the AuC6-NPs to leave the water/air or water/decane interfaces.

Due to limitations in the area range coverage in a single growing and shrinking experiment, several growing and shrinking experiments were performed with different AuC6-NPs number at the interface in order to cover a wide range of AuC6-NPs per area of pendant drop. The surface pressure against the area per nanoparticle from the growing and shrinking pendant drop experiments are plotted in Fig. 4, for water/air and water/decane interfaces and for different AuC6-NPs concentrations.

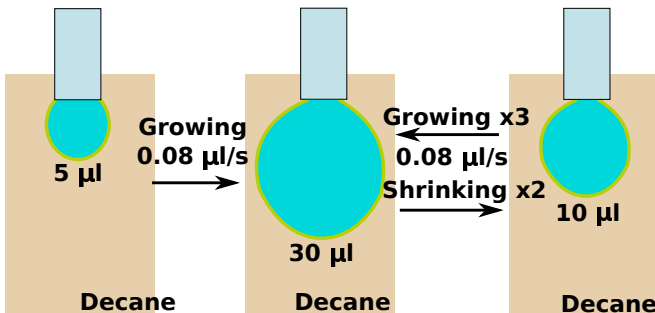
The particles exhibited a near zero electrophoretic mo-



(a) Diagram of AuC6-NPs deposition at the surface of a initial $5 \mu\text{l}$ MilliQ water pendant drop and subsequent growing at a $0.08 \mu\text{l/s}$ rate and up to $20 \mu\text{l}$.



(b) Growing and shrinking pendant drop experiment in water/air interface between $20 \mu\text{l} \leftrightarrow 10 \mu\text{l}$ at a $0.08 \mu\text{l/s}$ rate.



(c) Immersion of $5 \mu\text{l}$ water pendant drop with AuC6-NPs deposited at the interface and growing and shrinking pendant drop experiment in water/decane interface between $30 \mu\text{l} \leftrightarrow 10 \mu\text{l}$ at a $0.08 \mu\text{l/s}$ rate.

Figure 1: Diagram of deposition of AuC6-NPs at a water/air interface and subsequent growing and shrinking pendant drop experiments with water/air and water/decane interfaces.

bility (see Section II B). This affects to the models based in the repulsion between charged particles¹¹ which predict negligible surface pressures due to the low effective electric charge of the AuC6-NPs. Moreover, the relative short chains of the hexanethiol coverage of the AuC6-NPs are readily oriented rather than large polymers¹². In fact,

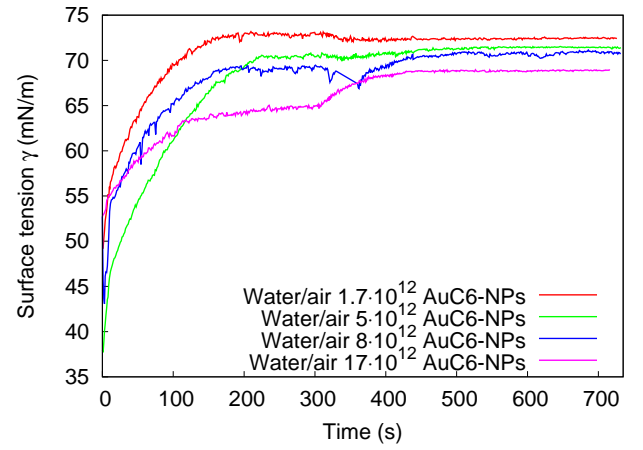


Figure 2: Surface tension against time when different number of AuC6-NPs in THF were deposited onto the MilliQ water pendant drop. The initial drop volume was $5 \mu\text{l}$ and it grew at $0.08 \mu\text{l/s}$ rate up to $20 \mu\text{l}$. After the THF evaporation, the surface tension remained stable. The error due to the calculation of the surface tension from each pendant drop profile was in the range of 1 mN/m and the room temperature was 25°C .

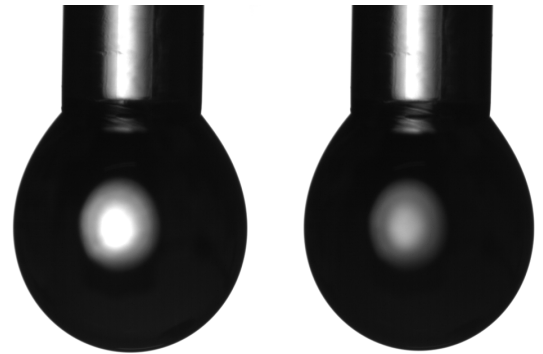


Figure 3: $10 \mu\text{l}$ MilliQ water pendant drop in air with $\sim 5 \cdot 10^{12}$ AuC6-NPs (left) and $\sim 17 \cdot 10^{12}$ AuC6-NPs (right).

the simply scaled particle theory of hard disks model¹⁰ (see Eq. 1) is in agreement with the experimental data for hard disks with 1 nm diameter (see Fig. 4).

$$\Pi(A_{particle}) = \frac{k_B \cdot T}{A_{particle} \cdot \left(1 - \frac{\pi \cdot d^2}{4 \cdot A_{particle}}\right)^2} \quad (1)$$

Equation 1 is written in terms of surface pressure Π against the area per particle at the interface $A_{particle}$, where k_B is the Boltzmann constant, T is the temperature and d is the hard disk diameter. The agreement between experimental results and the simply scaled particle theory of hard disks model (Fig. 4) was good with 1 nm diameter rather than 2 nm diameter of the AuC6-NPs. This result may point out that not all the AuC6-

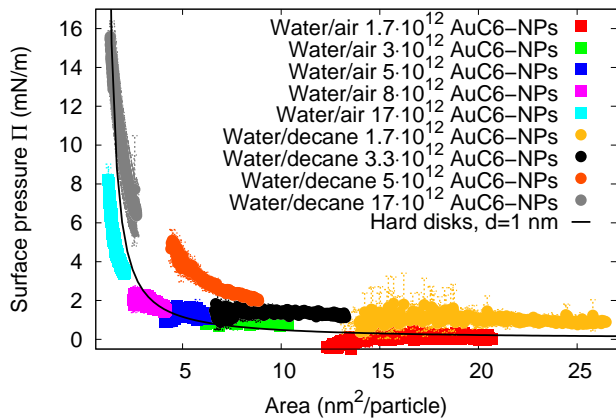


Figure 4: Surface pressure against the interface area of the pendant drop divided by the deposited AuC6-NPs number for water/air and water/decane interfaces and for different AuC6-NPs concentrations. The solid line is the hard disks model (Eq. 1) for disks of 1 nm diameter.

NPs deposited at the interface were really adsorbed at it. If the actual amount of AuC6-NPs was lower, then there was necessary less available area to get a close-packed arrangement and thus the hard disk model provide a lower effective diameter.

The hard disk behavior can be explained because at low concentrations there is not significant effect on the surface tension and at high concentrations (i.e. lower area per particle) the particles are near close-packed. Although the final amount of AuC6-NPs at the interface might not be equal to the nominal value, the low hysteresis of growing and shrinking experiments (see Section II C) might point out that the remaining AuC6-NPs

at the water/air or water/decane interfaces are effectively anchored to the interface. At the water/air interface, the hydrophobic character of the hexanethiol coverage of the AuC6-NPs can explain that the AuC6-NPs were successfully adsorbed at the interface. Instead, at the water/decane interface, the gold core may act as the hydrophilic part of an amphiphilic nanoparticle that is placed at the interface.

IV. CONCLUSIONS

The pendant drop technique was successfully used to characterize the interfacial activity of nanoparticles available in small amounts. The pendant drop technique was applied to 2 nm-diameter AuC6 nanoparticles at water/air and water/decane interfaces. The external deposition of the nanoparticles dispersed in tetrahydrofuran onto the water/air interface and the subsequent growing and shrinking experiments enabled to characterize the arrangement of the AuC6 nanoparticles at the interface, as the area per nanoparticle available on the pendant drop was changed. Finally, the results of surface pressure against area per AuC6 nanoparticle were in agreement with the simply scaled particle theory of hard disks model.

ACKNOWLEDGEMENTS

This study was supported by the by the “Junta de Andalucía” (projects P09-FQM-4698, P10-FQM-5977, P12-FQM-1443), the “Ministerio de Economía y Competitividad” (project MAT2011-23339) and by US National Science Foundation (DMR-0804049). Authors thank to Dr. J.A. Holgado-Terriza for the software Contacto[©] used for surface tension measurements.

¹ Á. Detrich, A. Deák, E. Hild, A. L. Kovács, and Z. Hórvölgyi, *Langmuir* **26**, 2694 (2010).
² J. Y. Kim, S. Raja, and F. Stellacci, *Small* **7**, 2526 (2011).
³ V. Sashuk, R. Holyst, T. Wojciechowski, and M. Fiałkowski, *J. Colloid Interface Sci.* **375**, 180 (2012).
⁴ S. Pradhan, L. Brown, J. Konopelski, and S. Chen, *J. Nanopart. Res.* **11**, 1895 (2009).
⁵ S. Pradhan, L. Xu, and S. Chen, *Adv. Funct. Mater.* **17**.
⁶ S. Ferdous, M. Ioannidis, and D. Henneke, *J. Nanopart. Res.* **13**, 6579 (2011).
⁷ T. M. Ruhlman, A. H. Gröschel, A. Walther, and A. H. E. Müller, *Langmuir* **27**, 9807 (2011).
⁸ A. Torcello-Gómez, A. Jódar-Reyes, J. Maldonado-Valderrama, and A. Martín-Rodríguez, *Food Res. Int.* **48**, 140 (2012).

⁹ V. Garbin, J. C. Crocker, and K. J. Stebe, *J. Colloid Interface Sci.* **387**, 1 (2012).
¹⁰ A. Santos, M. López de Haro, and S. Yuste, *J. Chem. Phys.* **103**, 4622 (1995).
¹¹ R. Aveyard, J. Clint, D. Nees, and V. Paunov, *Langmuir* **16**, 1969 (2000).
¹² L. Isa, E. Amstad, K. Schwenke, E. Del Gado, P. Ilg, M. Kroger, and E. Reimhult, *Soft Matter* **7**, 7663 (2011).
¹³ M. Brust, M. Walker, D. Bethell, D. J. Schiffrin, and R. Whyman, *J. Chem. Soc., Chem. Commun.* **7**, 801 (1994).
¹⁴ F. Montes Ruiz-Cabello, M. Rodríguez-Valverde, and M. Cabrerizo-Vílchez, *J. Adhes. Sci. Technol.* **25**, 2039 (2011).